Expected seismic velocity profile for the suggested borehole location in Visp

Jan Burjánek (SED, ETHZ) and Donat Fäh (SED, ETHZ)

Suggested location of the borehole is close to the two sites where the ambient noise array measurement were performed (Burjanek et al., 2010a), and temporary stations were deployed (Figure 1). Resulting velocity profiles of upper part are presented in Figures 2,3.

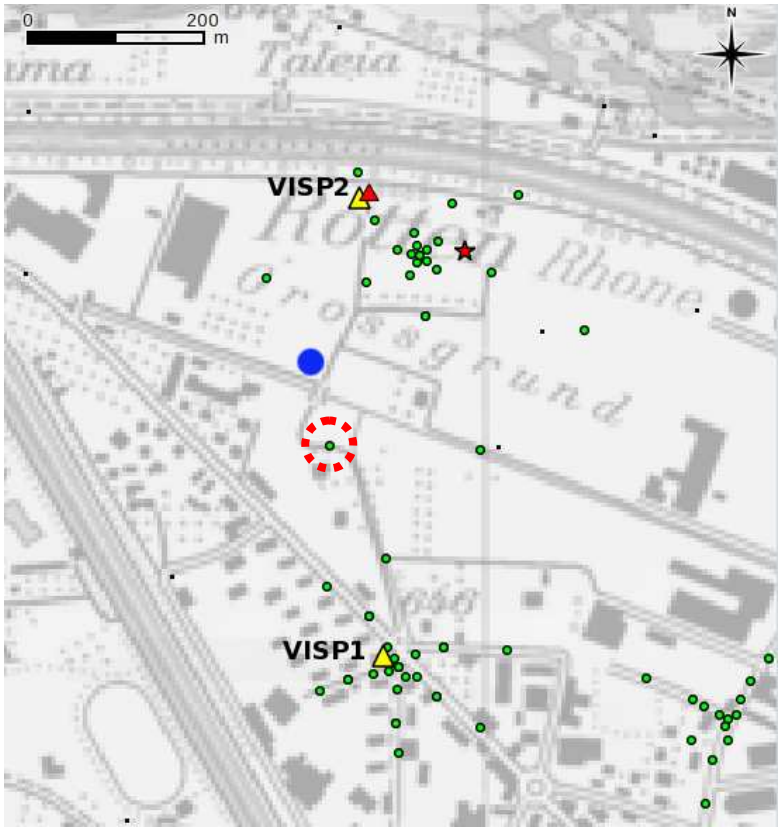

Figure 1*: Map of the area of interest – suggested borehole location (blue circle), temporary stations (yellow triangles), array measurements (green circles), new strong motion station (red triangle), active seismics (red star). The station in red circle is the closest site to the possible borehole location.*

It was not possible reach the bedrock depth with array measurements, the presented profiles are reliable down to 50-60m. The solutions obtained with 20 layers are preferred (black line in Figures 2,3). Both profiles then contain an interface around 50m. The velocities under VISP1 site are significantly higher above this interface.

Series of additional inversions were performed to constrain the bedrock depth by fitting the Rayleigh wave ellipticity curve. Particularly: 1) We fixed the velocity profile above the 50m interface. 2) Added to layers with both variable velocity and thickness bellow the 50m interface. 3) Fixed the S wave velocity of the bedrock to 2500m/s. The ellipticity curves were obtained by wavelet method (Fäh et al.,, 2009) from noise recordings made by temporary stations.

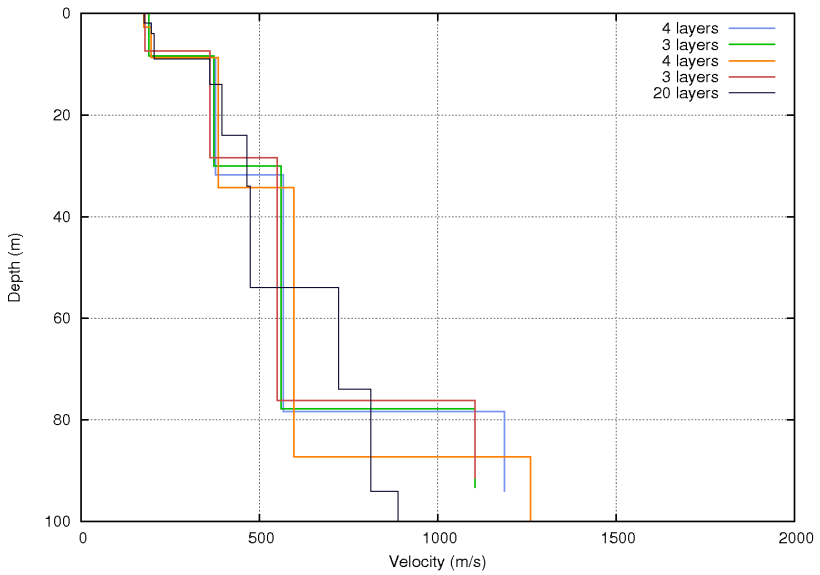

***Figure 2**: S wave velocity profiles for VISP1 site (array VIS4). Colors distinguish between different inversions (e.g., different parametrizations).*

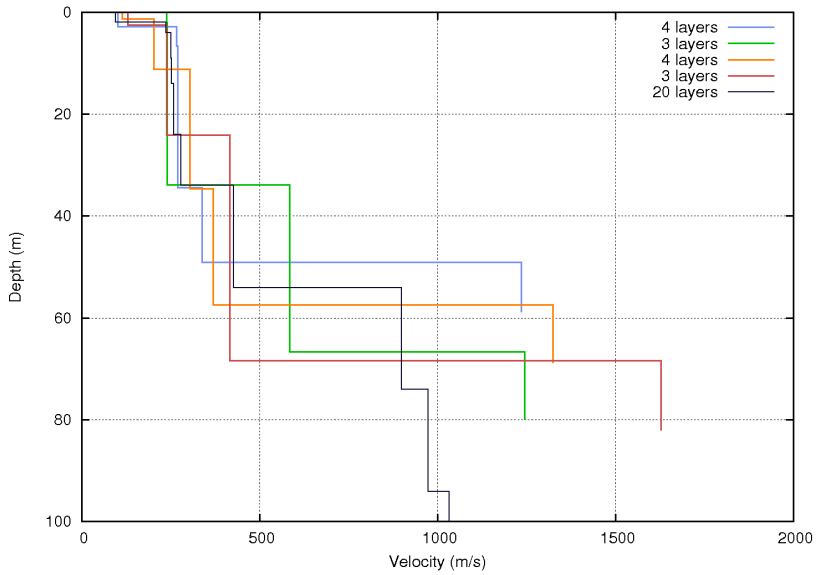

***Figure 3**: S wave velocity profiles for VISP2 site (array AVIS2). Colors distinguish between different inversions (e.g., different parametrizations).*

Concerning the site VISP1, observed ellipticity curve has a quite complex shape with no clear single peak (e.g., Figure 4). It was checked, that such complex shape of the ellipticity curve is stable in time (noise recordings of several days were analyzed). Several joint inversions of dispersion and ellipticity curves were performed for different relative weight between ellipticity and DC misfit. Contrary to previous inversions, we took into account also the points of the dispersion curves picked beyond the resolution limit of the array. The results of the joint inversions are plotted in Figures 4, 5, 6, with decreasing weight on ellipticity curve respectively. The resulting depth of the bedrock depends in this case on the weight we put on the ellipticity curve, ranging from 200m to 300m.

VISP1

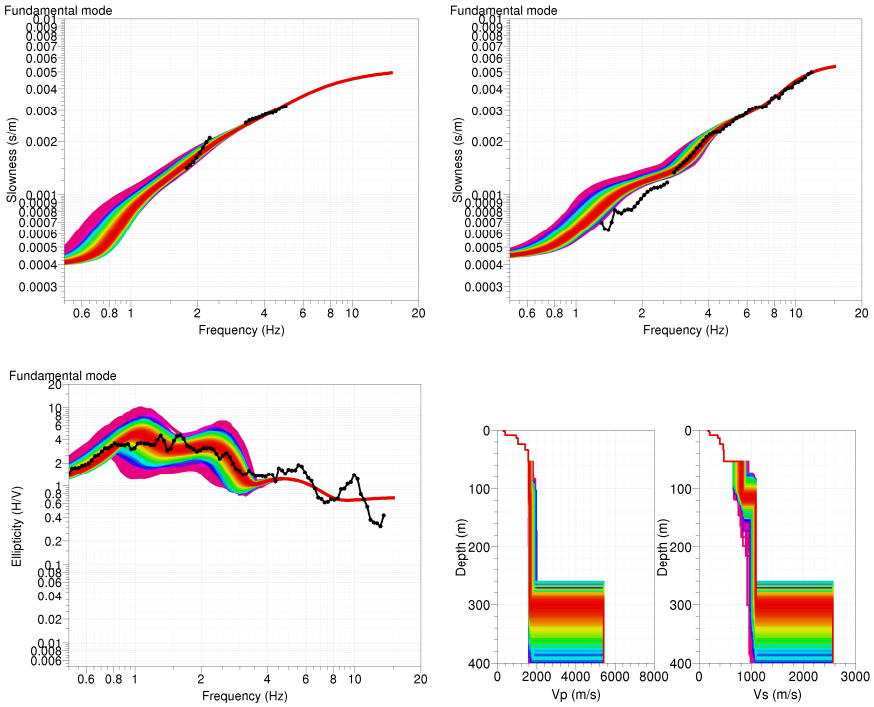

***Figure 4**: An ensemble of dispersion curves (Love – top left, Rayleight – top right), ellipticities (bottom left), and corresponding velocity profiles (bottom right). Observed curves used in the inversion are in black, the color distinguishes the misfit value. Substantial weight on the ellipticity curve was considered.*

VISP1

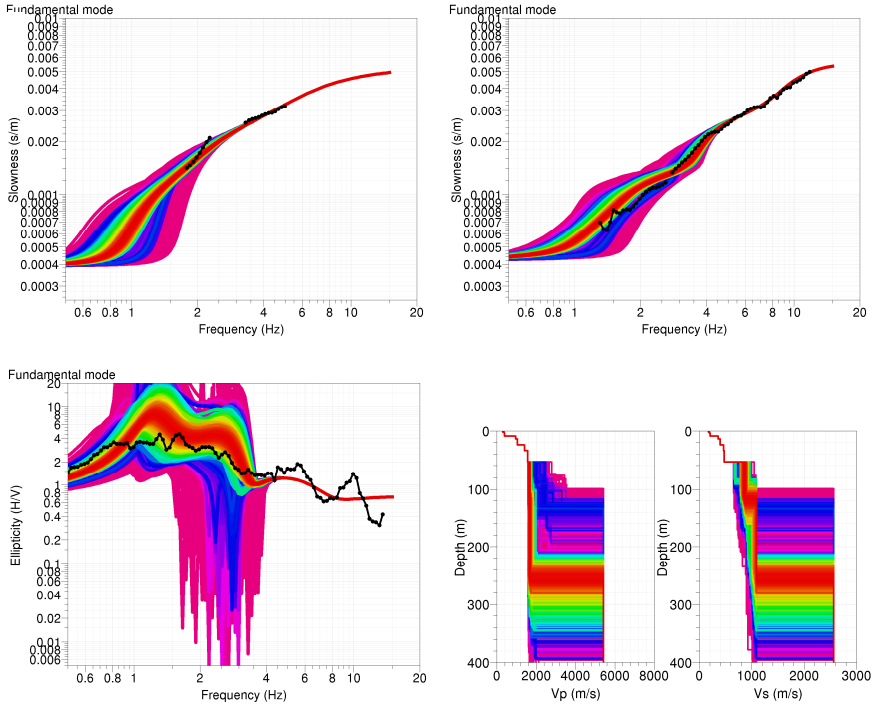

***Figure 5**: An ensemble of dispersion curves (Love – top left, Rayleight – top right), ellipticities (bottom left), and corresponding velocity profiles (bottom right). Observed curves used in the inversion are in black, the color distinguishes the misfit value. Moderate weight on the ellipticity curve was considered.*

VISP1

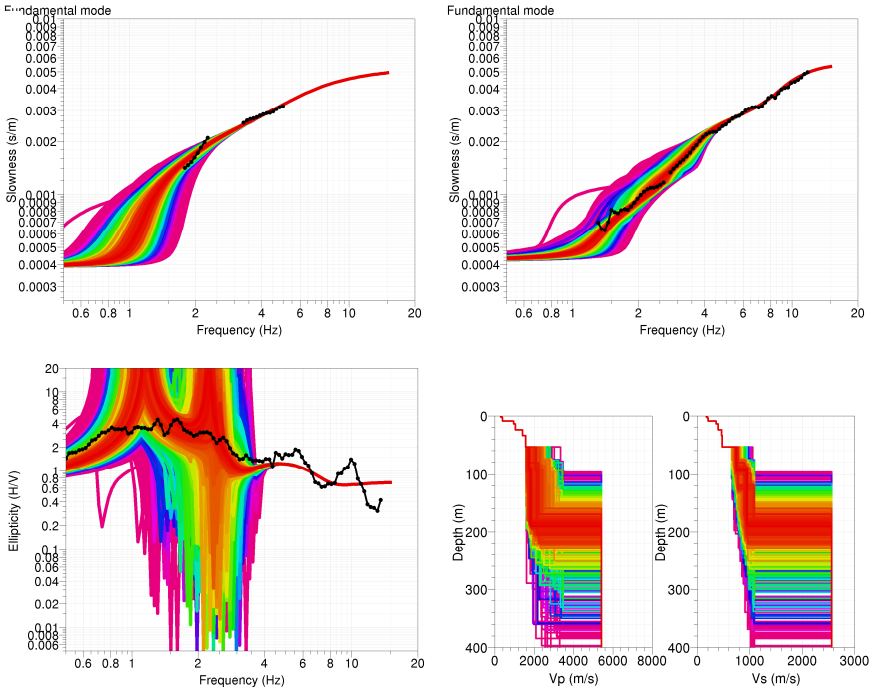

***Figure 6**: An ensemble of dispersion curves (Love – top left, Rayleight – top right), ellipticities (bottom left), and corresponding velocity profiles (bottom right). Observed curves used in the inversion are in black, the color distinguishes the misfit value. Low weight on the ellipticity curve was considered.*

VISP2

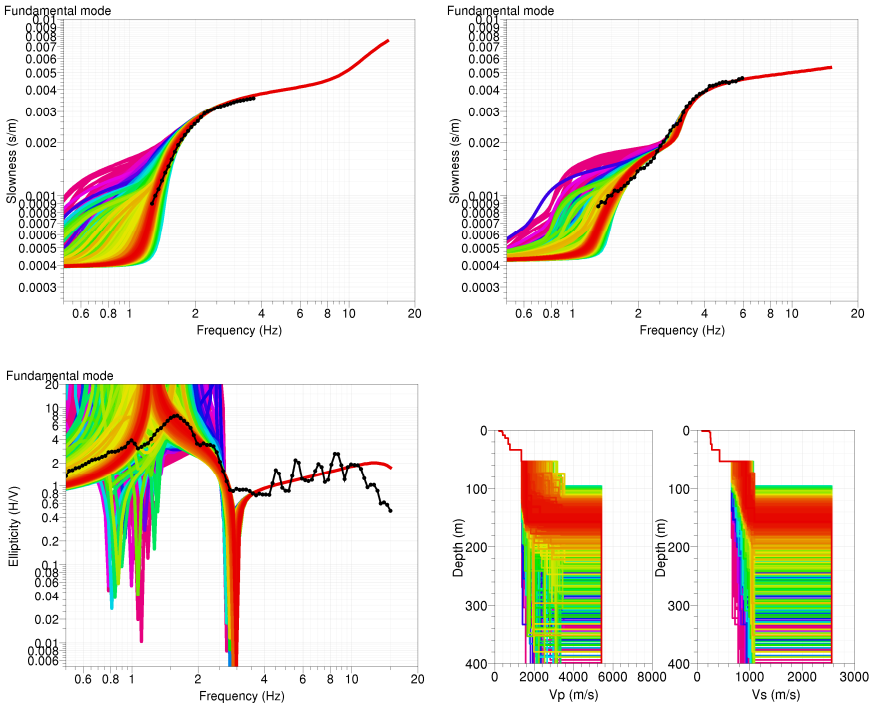

***Figure 7**: An ensemble of dispersion curves (Love – top left, Rayleight – top right), ellipticities (bottom left), and corresponding velocity profiles (bottom right). Observed curves used in the inversion are in black, the color distinguishes the misfit value. Moderate weight on the ellipticity curve was considered.*

Concerning the site VISP2, observed ellipticity curve has a simple shape with a clear single peak (e.g., Figure 7). The result of the joint inversion is plotted in Figure 7. In this case, the result is not so sensitive to the weight put on ellipticity. The bedrock depth is around 150m.

Finally, we compared site-to-reference spectral ratios (SRSR) obtained from recordings of regional earthquakes (Burjanek et al., 2010b) and synthetic S wave transfer functions (SH, vertical incidence) calculated for models presented above. In case of VISP1 site, the models with the deepest and shallowest bedrock (300m, 200m respectively) do not explain very well the observed SRSR. The model with the 250m bedrock is preferable for VISP1, since it fits at least the site fundamental frequency. In case of VISP2, synthetic transfer function is in quite good agreement with observed SRSR, so the average bedrock of 150m seems to be reasonable at this site.

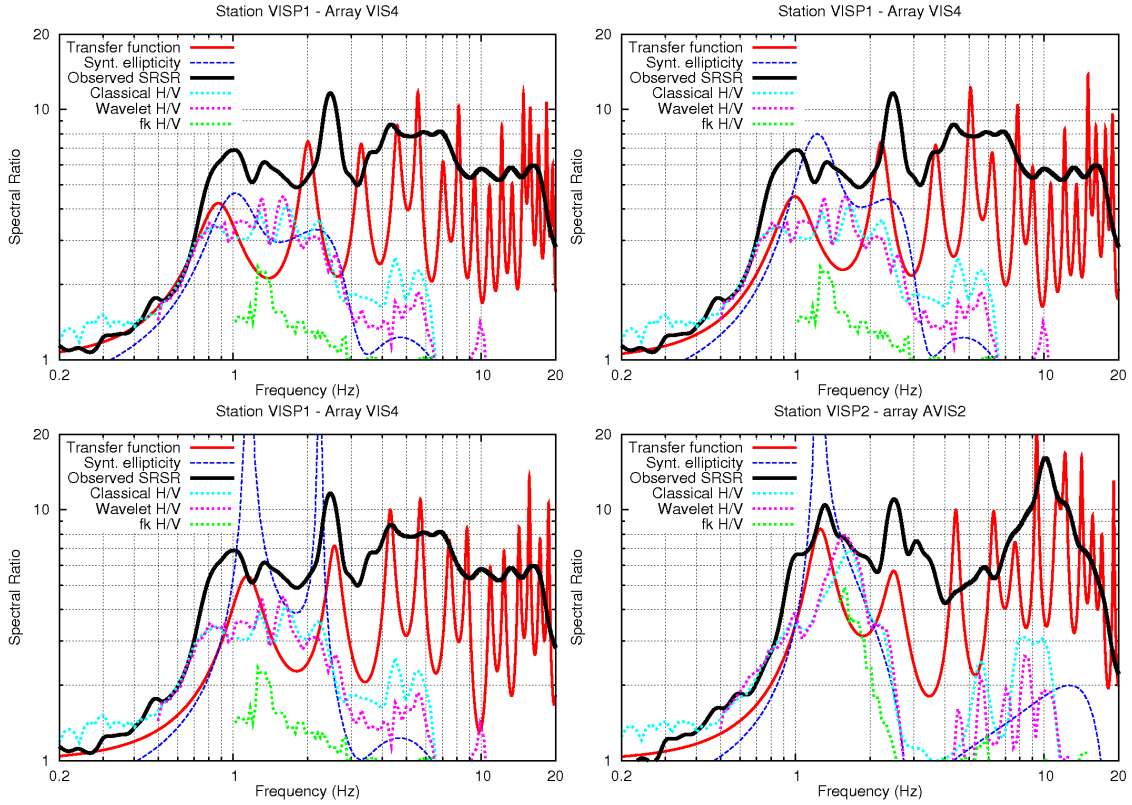

***Figure 8**: A comparison between observed site-to-reference spectral ratio (thick black) and synthetic S wave transfer function (red) for the following velocity profiles: best model from Figure 4 (here top left), best model from Figure 5 (here top right), best model from Figure 6 (here bottom left), and best model from Figure 7 (here bottom right). Synthetic ellipticity curves (dark blue), and estimated ellitpticity curves by different methods (classical method – light blue, wavelet method – violet, fk array method – green).*

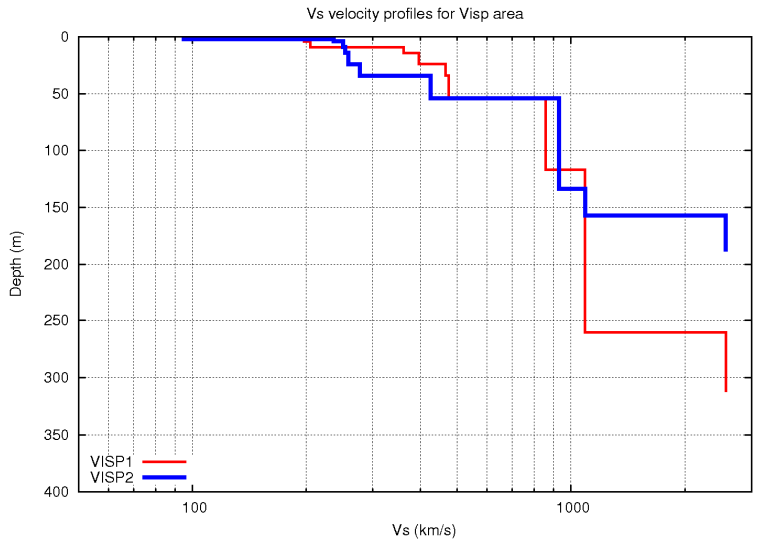

***Figure 9**: Estimated S wave velocity profiles for the VISP1 and VISP2 sites.*

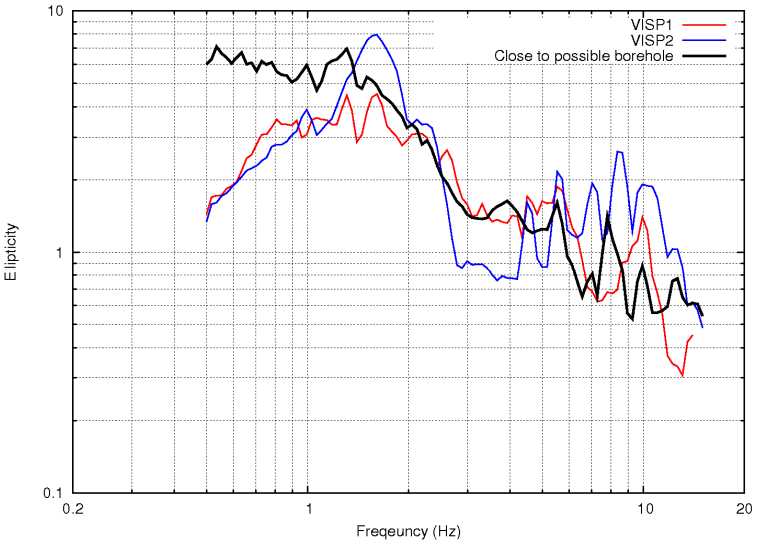

***Figure 10**: Comparison of observed ellipticity curves (obtained by wavelet method) – VISP1 (red), VISP2 (blue), and the array station closest to the possible borehole location (black), see Figure 1.*

Conclusions

The estimated velocity profiles are presented in Figure 9. The S wave velocity is in range of 100-500m/s in first 50m. S wave velocity then increases rapidly to 1000m/s at the depth of 50m. The depth of the bedrock (250m) is uncertain in case of VISP1.

Comparison of ellipticity curves from VISP1, VISP2, and the array station closest to the suggested borehole location is presented in Figure 10. This comparison indicates, that the velocity profile close to the possible borehole is closer to the one obtained for VISP1.

References

Burjanek, J., Gassner-Stamm, G., and Fäh, D. (2010a). Array - measurements in the area of Visp and St. Niklaus (COGEAR deliverable 3.1.2), Swiss Seismological Service, SED/COGEAR/R/003/20100226.

Burjanek, J., Gassner-Stamm, G., and Fäh, D. (2010b). Installation of semi-permanent seismic array and data analysis (COGEAR deliverable 3a.1.1.1), Swiss Seismological Service, SED/COGEAR/R/005/20100412.

Fäh, D., Wathelet, M., Kristekova, M., Havenith, H., Endrun, B., Stamm, G., Poggi, V., Burjanek, J., Cornou, C., (2009). Using Ellipticity Information for Site Characterisation, NERIES JRA4 “Geotechnical Site Characterization”, taskB2-D4, final report.

Additional array measurement

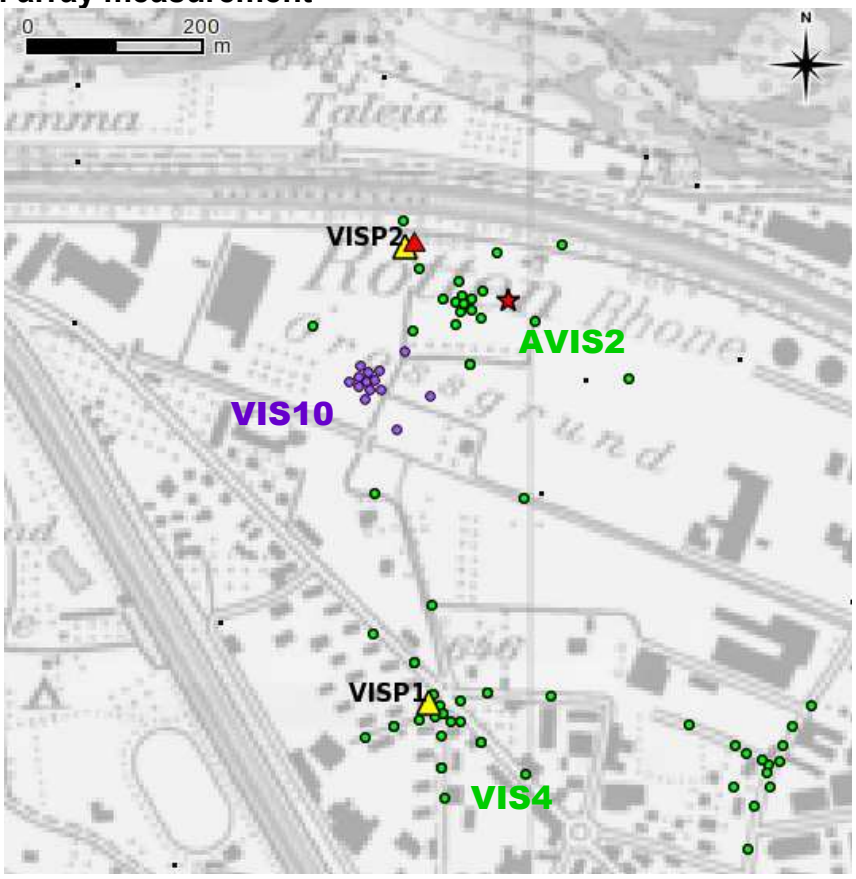

***Figure 12**: Map of the area of interest – additional array measurement VIS10 (violet circles).*

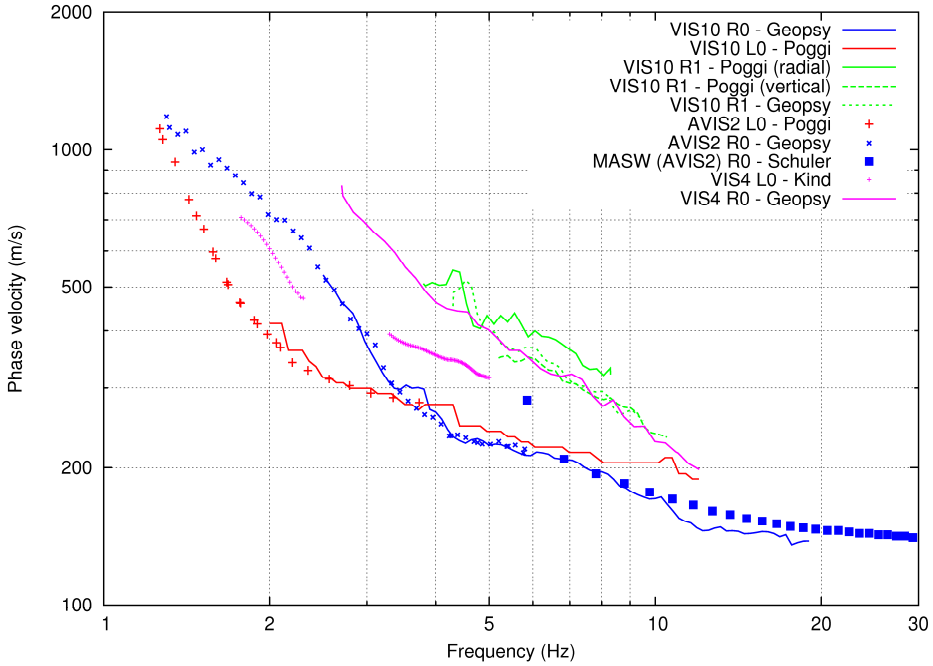

***Figure 13**: Comparison of dispersion curves from different surveys.*

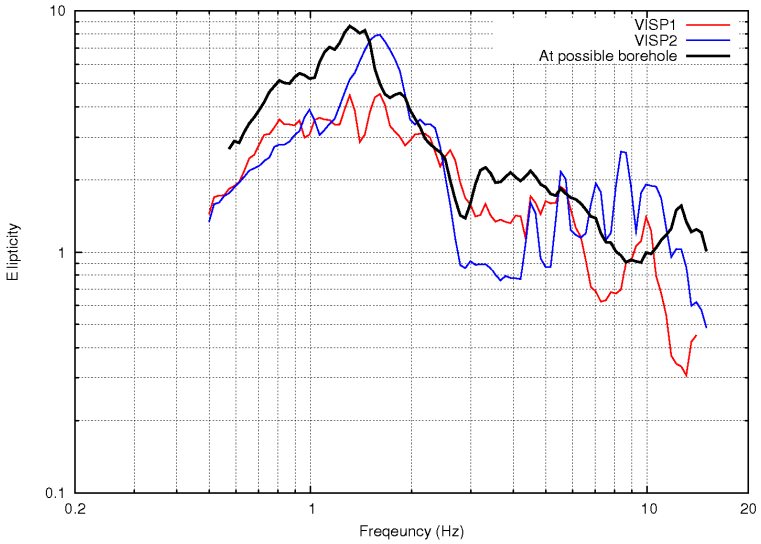

***Figure 14**: Comparison of observed ellipticity curves (obtained by wavelet method) – VISP1 (red), VISP2 (blue), VIS10 – average (black).*

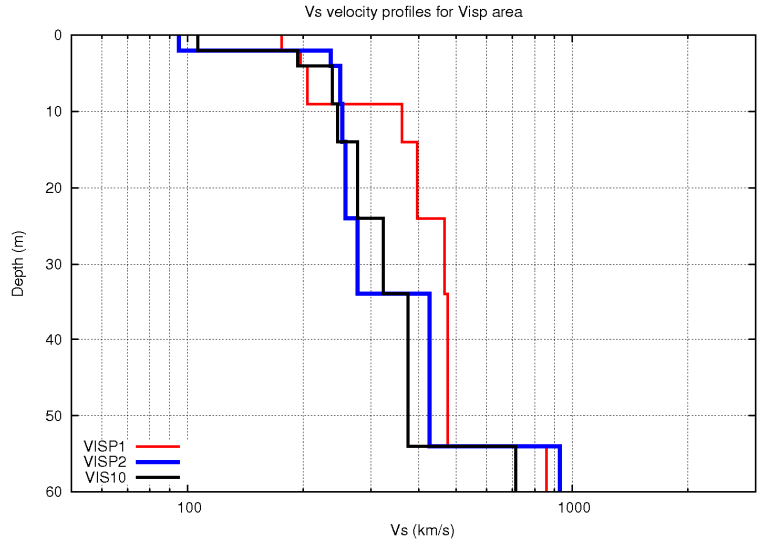

***Figure 15**: Estimated S wave velocity profiles for the VISP1, VISP2 and VIS10 sites.*

Dispersion curves obtained from the additional array VIS10 follow perfectly the dispersion curves from array AVIS2 and also the dispersion curves obtained by MASW. Consequently, S-wave velocity profiles are also very similar in upper part (Figure 15). Finally, Poisson ratio profiles are presented in Figure 16. The uppermost structure (<10m) is characterized by low Poisson ratio. Poisson ratio is over 0.4 bellow 10m (possible water table) and drops again around 50m (possible impermeable interface).

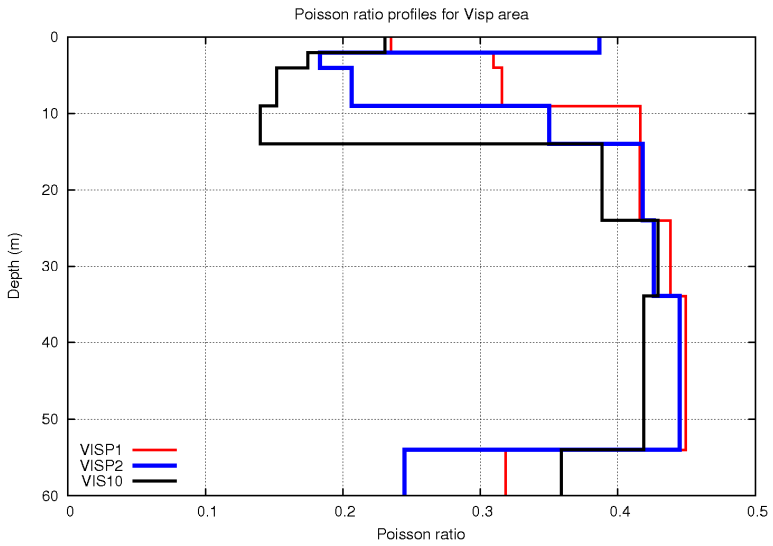

***Figure 16**: Estimated Poisson ratio profiles for the VISP1, VISP2 and VIS10 sites.*